Pergamon

SCIENCE DIRECT®

Tetrahedron 59 (2003) 5003–5018

TETRAHEDRON

Guaiazulene-based phenolic radical scavengers: synthesis, properties, and EPR studies of their reaction with oxygen-centred radicals

Emanuela Franchi,[a] Giovanni Ingrosso,[a,*] Fabio Marchetti[a] and Calogero Pinzino[b,*]

[a]*Dipartimento di Chimica e Chimica Industriale, Università di Pisa, Via Risorgimento 35, 56126 Pisa, Italy*
[b]*Istituto per i Processi Chimico-Fisici del C.N.R., Area della Ricerca di Pisa, Via G. Moruzzi 1, 56124 Pisa, Italy*

Received 20 February 2003; revised 14 April 2003; accepted 8 May 2003

Abstract—A variety of phenolic derivatives **4**, carrying the guaiazulene moiety, were prepared starting from guaiazulene. Compounds **4** react with oxygen-centred radicals exhibiting chromotropic behaviour. The radical scavenging power of these compounds was evaluated by different methods. Compounds **4** are less efficient than some of the most common radical scavengers but show quite selective behaviour towards different oxygen-centred radicals. A correlation is found between the antioxidant activity of the compounds **4** and the corresponding phenolic O–H bond dissociation energy. Some aspects of the reaction of the compounds **4** with oxygen-centred radicals were elucidated by EPR and DFT studies.

1. Introduction

Recent years have witnessed a great level of interest in the development of new compounds that allow us to prevent damage that can be associated with oxidative chain reactions induced by free radicals. Such processes can be inhibited or retarded by the addition of certain compounds known as 'antioxidants'.[1] The radical scavengers[2] are a particular class of antioxidants able to react with free radicals giving rise to a new radical species less reactive than its precursor, the original radical being transformed into a non-radicalic species. A wide variety of natural and synthetic compounds are known to exhibit powerful radical scavenging activity and, within these, sterically hindered phenols play a very important role.[2] Typically, the reaction of phenols with radicals implies a hydrogen transfer from the phenol to the reactive radical with the formation of the less reactive phenoxyl radical (Eq. (1)).[3]

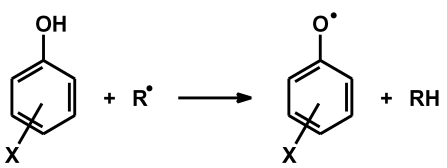

(1)

The electronic properties of a chromophoric group attached to the phenol skeleton, and then its absorption spectrum, may be markedly modified on passing from phenol to the corresponding phenoxyl radical. Thus, whenever the chromophoric group absorbs in the visible region, the phenol→phenoxyl transformation may be accompanied by a colour change. Radical scavengers of this type should then exhibit chromotropic behaviour on reaction with free radicals and, at least in principle, can be used to detect the presence of free radicals through a simple organoleptic or colorimetric approach.

We were attracted by the idea of synthesising new phenol-based radical scavengers having the above properties. In projecting the structure of the new compounds we were inspired by an interesting paper dealing with the detection of free radicals through their adducts with a guaiazulene-based nitrone **1**.[4]

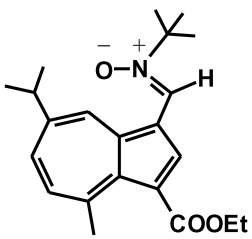

1

Guaiazulene, a deeply blue coloured alkyl derivative of azulene, appeared particularly promising as the chromophore to be introduced into the molecular skeleton of the desired phenol derivatives. Azulene and its derivatives have a remarkable dipole moments (μ=0.8–1.08 D) and unusual

Keywords: phenol derivatives; antioxidants; radical scavengers; guaiazulene; EPR; DFT calculations.

* Corresponding authors. vanni@dcci.unipi.it; rino@indigo.icqem.pi.cnr.it

0040–4020/03/$ - see front matter
doi:10.1016/S0040-4020(03)00737-3

photo-physical properties, and, as such, have attracted great interest in organic, inorganic, medicinal, theoretical, and industrial chemistry.[5]

We report here the synthesis of several new phenol derivatives of formula **4**, as well as an evaluation of their radical scavenging power, along with some mechanistic aspects of their reaction with oxygen-centred radicals. Brief reports on the preliminary results of this study have already been communicated.[6] A laboratory test for detecting the presence of free radicals based upon the use of the compounds **4** has been set up and patented.[7]

2. Results and discussion

2.1. Synthesis and properties of the compounds 4

The derivatives **4a**–**4j** were prepared, according to Scheme 1, by reacting the readily available acyl bromide **3**, which derives from guaiazulene **2**,[4] with a variety of dihydroxybenzene derivatives. All the compounds were obtained in moderate yields (20–50%), the main side product being in all cases the diesters of general formula **5** whose formation can be limited if the reaction is carried out by adding slowly the acyl bromide **3** to an ethereal solution of the appropriate dihydroxybenzene, at −30°C.

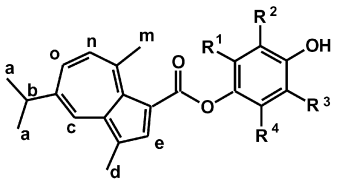

4

4a: $R^1 = R^2 = R^3 = R^4 = H$;
4d: $R^1 = R^3 = R^4 = H$, $R^2 = CH_3$;
4e: $R^1 = CH_3$, $R^2 = R^3 = R^4 = H$;
4f: $R^1 = R^3 = R^4 = H$, $R^2 = Bu^t$;
4g: $R^1 = Bu^t$, $R^2 = R^3 = R^4 = H$;
4h: $R^1 = R^2 = CH_3$, $R^3 = R^4 = H$;
4i: $R^1 = R^3 = H$; $R^2 = R^4 = Bu^t$,
4j: $R^1 = R^2 = R^3 = R^4 = F$;

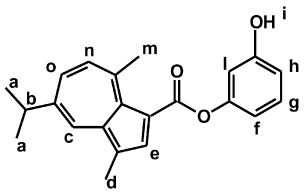

4b

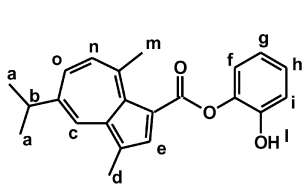

4c

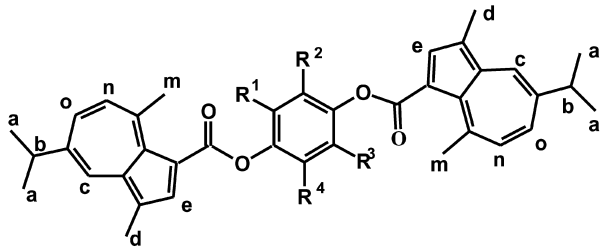

5a: $R^1 = R^2 = R^3 = R^4 = H$;
5f: $R^1 = R^3 = R^4 = H$, $R^2 = Bu^t$;
5h: $R^1 = R^2 = CH_3$, $R^3 = R^4 = H$;
5i: $R^1 = R^3 = H$; $R^2 = R^4 = Bu^t$,
5j: $R^1 = R^2 = R^3 = R^4 = F$;

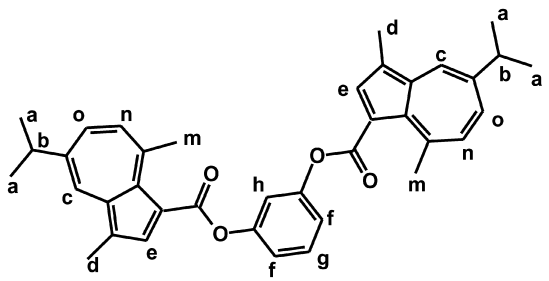

5b

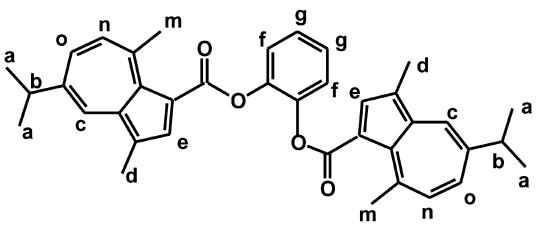

5c

Compounds **4** and **5** were fully characterized by elemental analysis, ^1H NMR, and, in the case of **4j**, also by ^{19}F NMR. The isomers **4d**–**4g** were unequivocally identified by means of NOE measurements.

With the aim of showing differences and analogies between the role played by the guaiazulene moiety and that played by other carbocyclic moieties in influencing the antioxidant

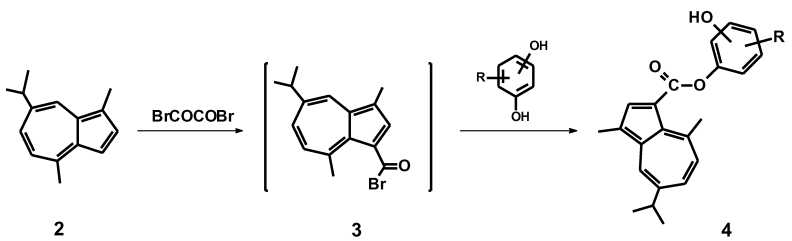

2 **3** **4**

Scheme 1.

properties of the resulting phenolic derivatives, compounds **6** and **7**, which contain the phenyl and the 1-naphthyl moieties, respectively, were prepared.

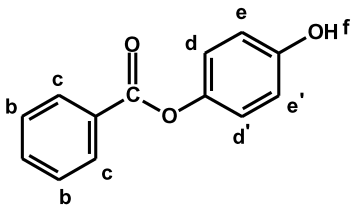

6

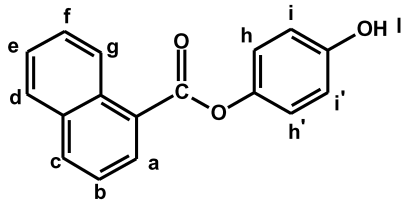

7

Like other phenol derivatives,[2] compounds **4** react with some oxygen-centred radicals (Scheme 2). Owing to their insolubility in water, all the experiments were carried out in an aqueous solution of *n*-decyl sulfate sodium salt (1 M). The tests involving H_2O_2 as the oxidant were carried out at pH≈4 using 2 M H_2O_2 solutions. No reaction takes place when the compounds **4** are dissolved in a O_2-saturated micellar medium, either in the presence or in the absence of $[Cu(en)_2][ClO_4]_2$ (0.01 M), or are reacted with H_2O_2 in the absence of any metal redox couple. Indeed, no colour variation occurred within 15 min. Moreover, TLC analysis of the reaction mixtures revealed only the presence of the starting guaiazulene derivative. Instead, a fast reaction takes place when compounds **4** are reacted with the Fenton-like system $[Cu(en)_2][ClO_4]_2/H_2O_2$,[8] that, as well known,[9] gives rise to the hydroperoxyl ($HOO^{\cdot}$), superoxide ($O_2^{-\cdot}$), and hydroxyl ($HO^{\cdot}$) radicals: the blue colour of the reaction mixtures disappears within 15 min, turning first red, then pale orange, and, finally, pale yellow. The reactivity towards the superoxide radical was tested by reacting the compounds **4** with a 0.1 M solution of KO_2 in dimethylsulphoxide (DMSO) in the presence of 18-crown-6 (0.1 M).[10] No colour variation was observed in any case. The observed chemical inertness towards the superoxide radical seems to indicate that, in the simultaneous presence of $HOO^{\cdot}$, $O_2^{-\cdot}$ and $HO^{\cdot}$, the guaiazulenic derivatives **4** are able to react fast only with the hydroxyl radical. This is interesting at least within some contexts as in the case of fibre bleaching by hydrogen peroxide-based products. In such a case, in fact, while the superoxide and its conjugate acid $HOO^{\cdot}$ seems to be essential for the bleaching process, the hydroxyl radical is highly undesired, it being responsible for the degradation of the fibre.[11] In this connection, it is interesting to underline that 2,6-di-*tert*-butyl-4-hydroxytoluene (BHT) exhibits only a moderate selectivity on reacting with various oxygen-centred radicals, under the same experimental conditions as above. In fact, BHT is not totally inert towards KO_2 in DMSO.

On the basis of the above findings, a simple laboratory test has been set up, based upon the use of the compounds **4**, for detecting the presence of oxygen-centred free radicals in micellar media, simply by observing a colour change.[7]

Quite surprisingly, when dissolved in an aqueous solution of *n*-decyl sulfate sodium salt (1 M; pH=9), i.e. under the same experimental conditions as above, compounds **6** and **7** undergo a slow hydrolytic reaction leading to the formation of hydroquinone and of the conjugate bases of the corresponding acids. Instead, **6** and **7** are stable in acidified *n*-decyl sulfate sodium salt surfactant (pH=4). Thus, it was possible to test their reactivity towards oxygen-centred radicals in such a medium. The results of these experiments show that both **6** and **7** exhibit very poor scavenging power towards the oxygen-centred radicals derived from the Fenton reaction, if compared with the compounds **4**. Indeed, TLC of the reaction products revealed that both **6** and **7** remained unchanged within the adopted reaction time (15 min). An interesting qualitative conclusion is that the presence of the guaiazulenic moiety in the compounds **4** not only confers chromotropic behaviour but also makes the ester bond less prone to basic hydrolysis.

The qualitative results concerning the reactivity of the compounds **4** with some of the most common oxygen-centred radicals prompted us to try to evaluate quantitatively their radical scavenging power towards specific radical species. To do this some of the published methods were adopted as described in the literature or slightly modified to take into account the properties (solubility and spectroscopic features) of compounds **4**. In particular, the method of the inhibition of the autoxidation of linoleic acid[12,13] allowed us to evaluate their peroxyl radical scavenging power in a micellar system. Moreover, some of the compounds **4** were also tested with the oxygen uptake method[14] which allowed us to evaluate their peroxyl radical scavenging power in a homogeneous organic

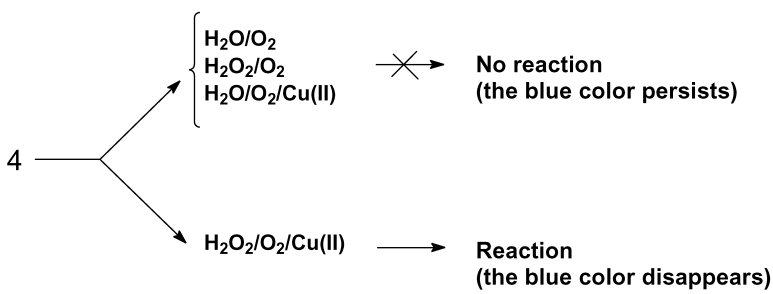

Scheme 2.

medium. Finally, by using an appropriately modified version of the inhibition of the degradation of deoxyribose method,[15,16] the radical scavenging efficiency of **4a**–**4j** towards the hydroxyl radical[17] was evaluated.

The evaluation of the rate for the autoxidation of linoleic acid to the corresponding conjugated diene hydroperoxide (Eq. (2)), both in the absence and in the presence of an antioxidant, constitutes a convenient method for measuring the efficiency of a given compound in scavenging peroxyl radicals in a micellar medium.[12] This is based on the recording the variation of the UV absorbance (λ=234 nm) of the hydroperoxide vs time.

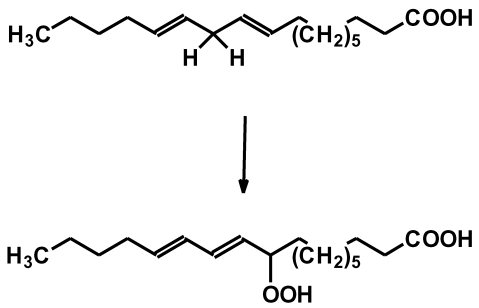

(2)

Accordingly, an aqueous buffered (pH=7.4) solution containing linoleic acid (2.6×10^{-3} M) and sodium *n*-dodecyl sulfate (0.1 M) was reacted with 2,2′-azobis(2-amidinopropane)hydrochloride (ABAP) as radical initiator, under air atmosphere at 37°C. The mathematical treatment of the experimental data was performed exactly as reported in the literature.[12] The resulting relative antioxidant efficiency (RAE) of the compounds **4a**–**4i** and of BHT are summarized in Table 1.

The RAE values show that the compounds **4a**–**4i** are markedly less efficient than BHT as far as their peroxyl radical scavenging power in a micellar system is concerned. In particular, three different behaviours can be envisaged depending upon the position and the nature of the phenolic substituents. The relative antioxidant efficiency of **4d**,**4f**,**4h** and **4i** can be evaluated with a reasonable accuracy. The compounds **4c**,**4e** and **4g** show, instead, too lower inhibition power to be quantitatively measured. Finally, the other radical scavengers are completely inert towards the peroxyl radicals. Thus, the data show clearly that the most efficient radical scavengers have at least one alkyl substituent at the *ortho* positions (compounds **4d**,**4f**,**4h** and **4i**). Interestingly,

Table 1. Relative antioxidant efficiency of the compounds **4a**–**4i** and BHT and rate constants for the inhibition of the autoxidation of linoleic acid by compounds **4d**,**4f**,**4h** and **BHT**

Radical scavenger	RAE	Error (%)	$k_{inh}\times10^{-4}$ (M^{-1} s^{-1})
BHT	0.26	10	1.04
4f	0.056	20	0.22
4d	0.040	2	0.16
4i	0.025	8.6	0.10
4h	0.0077	3	0.03
4e	Very low	–	–
4g	Very low	–	–
4c	Very low	–	–
4a	No inhibition	–	–
4b	No inhibition	–	–

the radical scavengers **4h** and **4i**, which carry also an alkyl group at the *meta* positions, show lower RAE values, and the compounds **4e** and **4g**, which carry only one *meta* alkyl group, exhibit very low scavenging power. Finally, the least efficient radical scavengers are the compounds **4a** and **4b**, both containing an unsubstituted phenolic rings which undoubtedly have a lower electron density than all the others because of the lack of the positive inductive effect exerted by the alkyl groups. It is indeed well known[18] that the electron density on the phenolic ring is markedly influenced by the position and the electron donor–acceptor properties of its substituents, *ortho* and *para* substitution being much more effective. Since radicals are electrophilic species, a phenolic ring will be more susceptible to the attack by such species, i.e. will be activated, if it carries electron-donating substituents. On the other hand, the presence of electron-withdrawing substituents on the phenolic ring plays, expectedly, the opposite role.

Starting from the RAE value it is possible to calculate the absolute value of the inhibition rate constant k_{inh} of a given radical scavenger.[12] In fact, the multiplication of the RAE value by the absolute rate constant for the reaction of peroxyl radicals with α-tocopherol, converts the RAE value into the absolute value of k_{inh} for each inhibitor. The value of k_{inh} for α-tocopherol in this micellar system has been measured by Barclay et al.[19] and found to be 4×10^{4} M^{-1} s^{-1}. The calculated values for the rate constant for the inhibition of the autoxidation of linoleic acid by compounds **4d**,**4f**,**4h**,**4i** and BHT are reported in Table 1. Interestingly, the inhibition rate constant we find in the case of BHT (1.04 M^{-1} s^{-1}) agrees very well with the reported value (1.1 M^{-1} s^{-1}).[20]

The above results led to two main questions. Do compounds **4** have an intrinsically low peroxyl radical scavenging activity? Does their activity depend markedly upon the reaction medium? Thus, we were keen to evaluate the antioxidant activity of some of the compounds **4** toward peroxyl radicals in a non-micellar homogeneous solution. This was done by adopting the oxygen up-take method that is based on the direct recording of the dioxygen consumption using a highly sensitive pressure transducer, during the inhibition of an autoxidation process. This method, set up by Ingold and co-workers[14] to evaluate the styrene polymerisation inhibition rate, is now largely employed in various systems. Thus, we studied the inhibition of cumene autoxidation to cumylhydroperoxide by some compounds **4** in cumene itself. The measurements were carried out at 50°C monitoring the variation of oxygen concentration during the inhibition of the autoxidation of cumene initiated by 2,2′-azo-bis(isobutyronitrile) (AIBN) (2.95×10^{-3} M). Four sets of experiments were run using the compounds **4a**,**4c**,**4i** and **4j**. Two types of kinetic profiles were observed: the behaviour of **4i** is quite similar to that observed for α-tocopherol (Fig. 1), while those shown by the other compounds look like that of BHT (Fig. 2). These results are the consequence of the different efficiency of these compounds in the peroxyl scavenging activity; in particular in the case of the experiments reported in Figure 2, the steady-state kinetic analysis could not be applied owing to the existence of competitive reactions. For this reason, two different kinetic mathematical treatments were carried out.

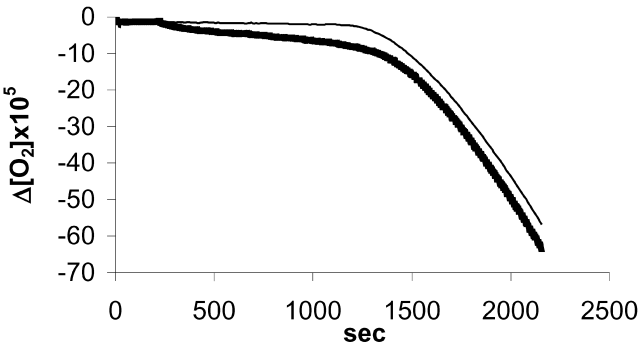

Figure 1. Dioxygen up-take (*M*) during the autoxidation of cumene inhibited by α-tocopherol (—) and by **4i** (▬) vs time; *T*, 50°C; concentration of the radical scavenger, 5×10^{-3} mM; concentration of the initiator, 3×10^{-3} M.

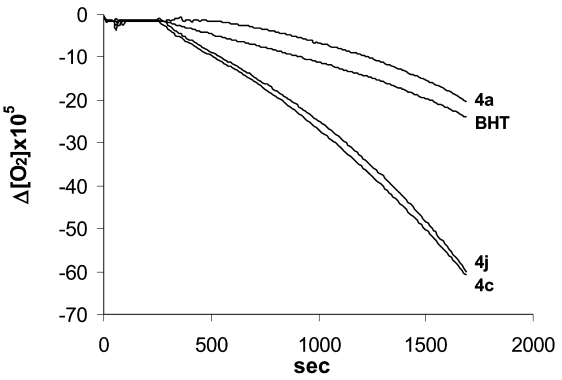

Figure 2. Dioxygen up-take (*M*) vs time during the inhibition of cumene autoxidation by **BHT**, **4a**,**4c** and **4j**; *T*, 50°C; concentration of the radical scavenger, 5×10^{-3} mM; concentration of the initiator, 3×10^{-3} M.

In the first case (Fig. 1), the value of the inhibition rate constant for the reaction of **4i** with peroxyl radicals, i.e. k_{inh} (16×10^4 M^{-1} s^{-1}), was calculated according to the procedure reported in literature.[21] Furthermore, owing to the fact that the experimental curves relative to **4i** and to α-tocopherol have quite similar shapes, one can conclude that the stoichiometric factor (SF) for the reaction involving **4i**, that was assumed to be 2 as verified for α-tocopherol, is indeed not very distant from this value (1.98).[12] From the data reported in Figure 2, it was possible to calculate k_{inh} (5.3×10^4 M^{-1} s^{-1}) only for the inhibition reaction by compound **4a**, using a computational program[22] which integrates all the kinetic equations involved in the inhibition process. On the other hand, compounds **4c** and **4j** have very poor autoxidation power. The different behaviour of compound **4c**, if compared with that of **4a**, can possibly be accounted for by considering that the hydroxyl group in **4c** is too sterically hampered to be approached by the cumyloxyl radical. On the other hand, the behaviour of **4j** confirms that the presence of electron-withdrawing groups over the phenolic ring results in a marked decrease of the radical scavenging efficiency.

On the basis of all the results obtained for the inhibition of autoxidation process by compounds **4**, some conclusive considerations about the role played by the media reaction in the scavenging activity may be reported. In Table 2 a comparison between the k_{inh} values in cumene and in SDS is reported.

Table 2. Rate constants for the inhibition of linoleic acid and cumene autoxidation by α-tocopherol, BHT, and compounds **4a** and **4i**

Radical scavenger	k_{inh} (M^{-1} s^{-1}) (Homogeneous medium) (50°C) Cumene autoxidation	k_{inh} (M^{-1} s^{-1}) (Micellar medium) (37°C) Linoleic acid autoxidation
α-Tocopherol	n.d.	4×10^4
BHT	3.4×10^4	1.0×10^4
4i	16×10^4	0.1×10^4
4a	5.3×10^4	Too low to be evaluated

Some interesting conclusions can be drawn from the tabulated data. First, in all cases the peroxyl scavenging efficiency decreases on going from homogeneous organic medium to micellar medium, as already observed,[23] although no dramatic variation of k_{inh} is observed in the case of BHT on passing from the micellar medium to homogeneous organic medium, according to the literature.[20] Instead, the guaiazulene derivative **4a**, that is almost inactive in micellar medium, shows a peroxyl scavenging activity slightly higher than that of BHT in homogeneous medium, and a much more marked activity increase is observed in the case of **4i**. This is 10 times less active than BHT in micellar medium, and five times more active than BHT in homogeneous medium. Finally, we would underline that although the inhibition rate constants were calculated from experiments carried out at different temperatures, the observed differences cannot be accounted for only on this basis.

The $HO^{\cdot}$ scavenging power of the compounds **4** was tested by a very simple and largely employed method based upon the inhibition of the deoxyribose degradation.[15,16] Accordingly, $HO^{\cdot}$ radicals are generated by a classical Fenton reaction and reacted with 2-deoxy-D-ribose which undergoes an oxidative degradation reaction which results in the formation of malondialdehyde (MDA). On reaction with thiobarbituric acid (TBA), MDA gives rise to a pink adduct which absorbs at 532 nm ($\varepsilon=1.54\times10^5$ M^{-1} cm^{-1}) (Eqs. (3)–(5)).

$$Fe^{2+} + H_2O_2 \rightarrow OH^- + OH^{\cdot} + Fe^{3+} \quad (3)$$

$$OH^{\cdot} + \text{Deoxyribose} \rightarrow \text{Malonaldehyde} \quad (4)$$

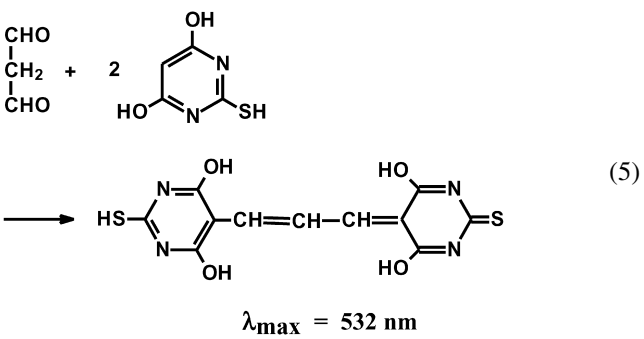

(5)

$$\lambda_{max} = 532 \text{ nm}$$

The extent of the formation of this adduct can be evaluated through UV–vis measurements. When a radical scavenger is added to the reactive system, it can compete with

Table 3. OH-Scavenging activity of derivatives **4a**–**4j** and BHT

Radical scavenger	OH-SA[a] (%)	Error (%)
BHT	47.7	5.5
4i	46.2	2.2
4b	46.2	8.5
4d	38.4	5.7
4a	37.0	11.0
4	36.8	8.3
4h	34.7	2.9
4f	34.3	2.3
4e	34.1	4.2
4c	33.7	3.0
4j	4.0	2.5

[a] Each figure represents the average over three runs.

deoxyribose in the reaction with the hydroxyl radical, thus limiting the degradation process of the sugar and then limiting the formation of the MDA–TBA adduct. UV–vis measurements allowed us to evaluate the entity of the inhibition process by recording the decrease of the absorbance at 532 nm vs the absorbance of a reaction mixture not containing any radical scavenger. It was necessary to modify adequately the published experimental procedure[16] in consequence of the insolubility of the compounds **4** in water as well as of their spectroscopic peculiarities. Thus, the reactions were carried out in sodium *n*-dodecyl sulfate (0.1 M). Moreover, in order to avoid the interference of the absorption by the guaiazulenic moiety at 532 nm, the measurement of the absorption of a blank, containing only the reactive system and the radical scavenger, was necessary. The OH-Scavenging Activity (OH-SA) (Table 3) could be then determined through the Eq. (6).

$$\text{OH-SA} = \left\{1 - \frac{A_{(\text{R+S+TBA+TCAA})} - A_{(\text{R+S})}}{A_{(\text{R+TBA+TCAA})}}\right\} \times 100 \qquad (6)$$

where R indicates the reactive system: $FeSO_4{\cdot}7H_2O$, EDTA, 2-deoxyribose, phosphate buffer, H_2O_2; S refers to the radical scavenger; TBA is thiobarbituric acid; TCAA is trichloroacetic acid; $A_{(\text{R+S+TBA+TCAA})}$ is the absorbance of the inhibited system at 532 nm; $A_{(\text{R+S})}$ is the absorbance at 532 nm of the inhibited system not containing either TBA or TCCA, which correlates to the unreacted scavenger; $A_{(\text{R+TBA+TCAA})}$ is the absorbance of the uninhibited system at 532 nm.

The data in Table 3 show clearly that the compounds **4**, with the only exception of the fluorinated compound **4j**, are moderately less efficient than BHT in scavenging the hydroxyl radical. All of them exhibit indeed a radical scavenging power not higher than 46%. A main conclusion is then that the substitution of the phenolic ring has a little effect on the reactivity of the compounds **4** towards the hydroxyl radical. Only the fluorine derivative **4j** shows a very low radical scavenging power, which confirms the already observed effect caused by the presence of electron-withdrawing groups on the phenolic ring.

It is well known[3] that phenol derivatives react with free radicals undergoing the hydroxylic hydrogen transfer process, thus giving rise to the corresponding phenoxyl radical. It is thus expected that a low phenolic O–H bond dissociation energy (OH-BDE) should favour the hydrogen transfer process, although this is only one of the several parameters that influence the reaction.[24–26] As shown in the next section, we have acquired some evidence that the derivatives **4** exert their radical scavenging activity giving rise to the corresponding phenoxyl radicals. Thus, we tried to verify if a correlation exists between the antioxidant power of compounds **4** and their O–H bond dissociation energy, D(O–H). The DFT calculation of the D(O–H) for the compounds **4a**,**4c**,**4i** and **4j** was carried out with Spartan 5.1 program,[27] assuming that the difference in the solvating free energy between the phenolic derivative and the corresponding phenoxyl radical is independent of substitution. The energies E, E_R and E_H, from the optimised geometries at pBN/DN** level, were obtained for phenol derivatives, phenoxyl radicals, and hydrogen radicals, respectively. The phenolic O–H bond dissociation energy values were thus obtained from the equation $D(O–H)=E-E_R-E_H$ (Table 4).

It is apparent from the data of Table 4 that the bond dissociation energies of the examined guaiazulene derivatives decrease in the order **4i**<**4a**<**4c**<**4j**. Interestingly, the hydroxyl radical scavenging activity of these compounds (see Table 3) decreases in the same order. The fluorinated derivative **4j** exhibits the highest bond dissociation energy and, accordingly, a very poor radical scavenging activity. On the other hand, compound **4i** exhibits the lowest value of bond dissociation energy and is the most efficient scavenger of peroxyl radicals both in micellar and organic media, being almost five times more efficient that BHT in the latter medium (see Table 2).

Table 4. Bond dissociation energy of some phenolic derivatives

Radical scavenger	O–H Dissociation energy (kcal mol^{-1})
4a	84.9
4c	86.5
4i	80.4
4j	90.2
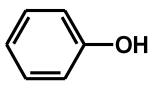	87.6[32]
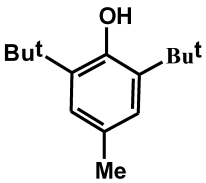 **BHT**	81.1[32]
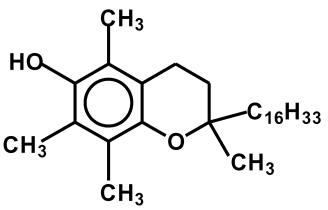 **α-tocopherol**	78.7[32]

Finally, a comparison of the O–H bond dissociation energies of the guaiazulenic derivatives with those reported in the literature for phenol, BHT, and α-tocopherol (see Table 4) points out clearly that BHT and α-tocopherol are indeed characterised by a lower bond dissociation energy value, while phenol, which is not a good antioxidant, has an O–H bond dissociation energy higher than those exhibited by the compounds **4a**,**4c** and **4i**.

2.2. Mechanistic aspects of the reaction of compounds 4 with oxygen-centred radicals: EPR and DFT studies

First of all, our efforts were directed to get evidence for the hypothesized formation of a transient phenoxyl radical on reaction of the compounds **4** with oxygen-centred radicals. At least in one case, i.e. by reacting **4i** with the H_2O_2/Cu(II) system, we succeeded in this. Indeed, operating at very low copper(II) concentrations (ca. 10^{-7} M) so as to avoid the appearance of the signal due to paramagnetic copper(II) centres, the EPR spectrum reported in Figure 3 was obtained, which shows a double doublet (g_{iso}=2.0042). This was nicely simulated[28] by best fitting to the experimental spectrum, with the optimisation of the hyperfine coupling constants (hfcc) and the line-widths. Thus, it was associated with the phenoxyl radical **8** (Eq. (7)) whose spin delocalisation extends almost exclusively over the phenolic ring, preferably over the *ortho* positions rather than over the *meta* ones, as indicated by the hyperfine coupling constant with *ortho*- and *meta*-hydrogen nuclei: $a_{H(ortho)}$=5.8 G; $a_{H(meta)}$=1.5 G.

Table 5. Selected experimental and (calculated) bond lengths (Å) of **4a** and **4b**

Compound **4a**		Compound **4b**[a]	
Bond	Length	Bond	Length
O(3)–C(20)	1.369(6) (1.3687)	O(3)–C(19)	1.355(9)
		O(6)–C(41)	(1.3683)
C(17)–O(1)	1.417(6) (1.3958)	C(17)–O(1)	1.404(8)
		C(39)–O(4)	(1.4090)
O(1)–C(1)	1.368(6) (1.3777)	O(1)–C(1)	1.349(8)
		O(4)–C(23)	(1.3921)
C(1)–C(2)	1.456(7) (1.4752)	C(1)–C(2)	1.456(9)
		C(23)–C(24)	(1.4748)

[a] The data refer to the two independent molecules present in the cell, and are given as the average over the parameters observed for the two independent molecules.

The above hfcc assignments were substantiated by DFT calculations of the electron spin densities starting from the optimised molecular geometry of the phenoxyl radicals. The molecular geometries of some derivatives of **4** and of the corresponding phenoxyl radicals were obtained from DFT data. Interestingly, the data reported in Table 5 show that a very high accord exists between the bond lengths calculated for **4a** and **4b** and those obtained by single-crystal X-ray analysis (Fig. 4).

Thus, the electron spin densities at the hydrogen atoms were calculated, and the isotropic hfcc were obtained through the Fermi contact interaction. The spin density map for the

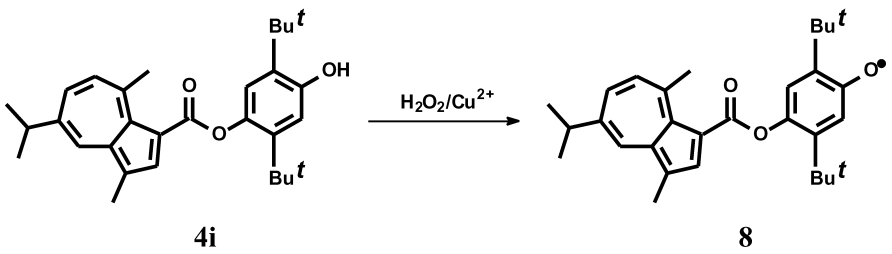

4i **8** (7)

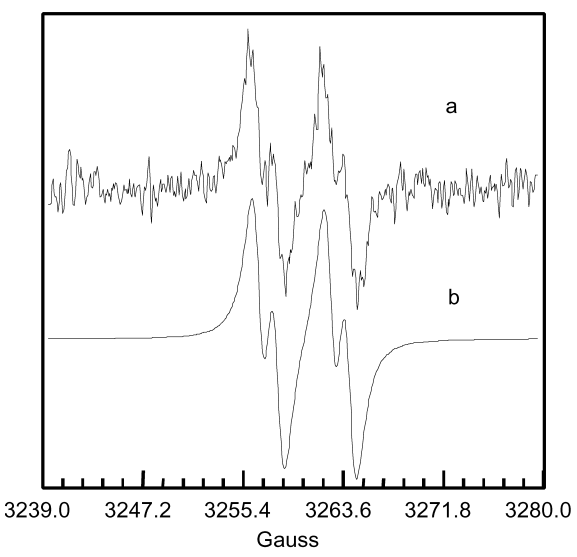

Figure 3. Experimental (a) and computer simulated (b) X-band EPR spectrum of the radical **8**, at 5°C.

radical **8** is shown in Figure 5. The hyperfine coupling constants calculated for the radical **8** ($a_{H(ortho)}$=5.5 G; $a_{H(meta)}$=1.5 G) are in a remarkable accordance with those obtained by computer simulation of the experimental spectrum.

The above EPR data strongly support the hypothesis that the reaction of the compounds **4** with oxygen-centred radicals implies first the abstraction of the hydroxylic hydrogen atom by the reacting radical, with the consequent formation of the corresponding phenoxyl radicals. A theoretical insight into the nature of the reaction between compounds **4** and free radicals came from DFT calculation of the electrostatic potential over the entire molecule as a consequence of the approaching of a positive charge, being the molecule considered to be isolated and in the gas phase. This appeared to us to be one of the best models to simulate the reaction of compounds **4** with an electrophilic species, like a free radical. The maps of the calculated electrostatic potential surfaces show clearly that all the guaiazulenic derivatives **4** exhibit very similar electronic distribution

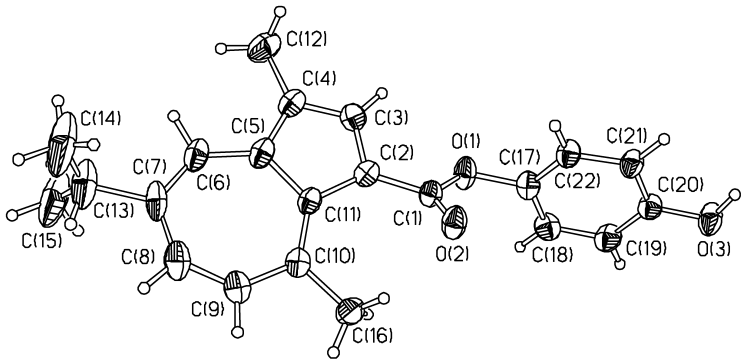

(a)

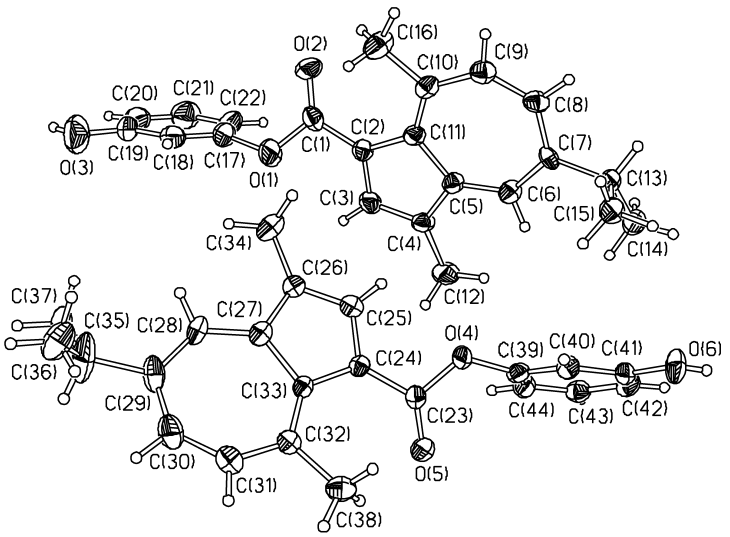

(b)

Figure 4. Molecular geometry of **4a** (a) and **4b** (b).

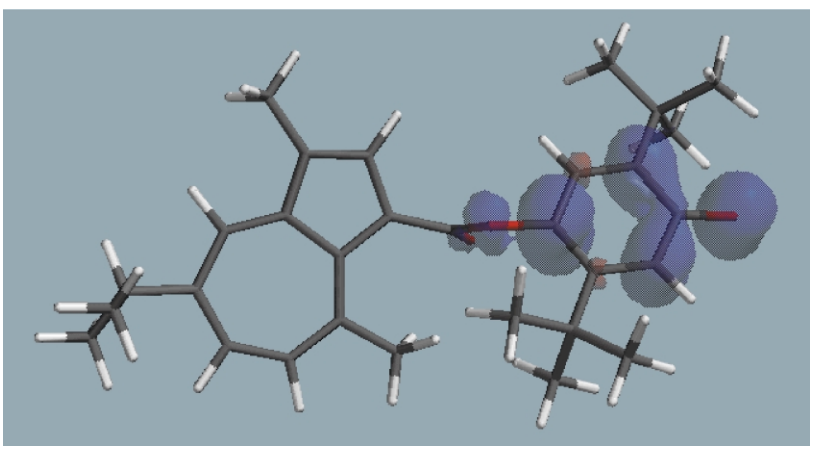

Figure 5. Calculated spin density surface (0.002 e au^{-3}) of the radical **8**.

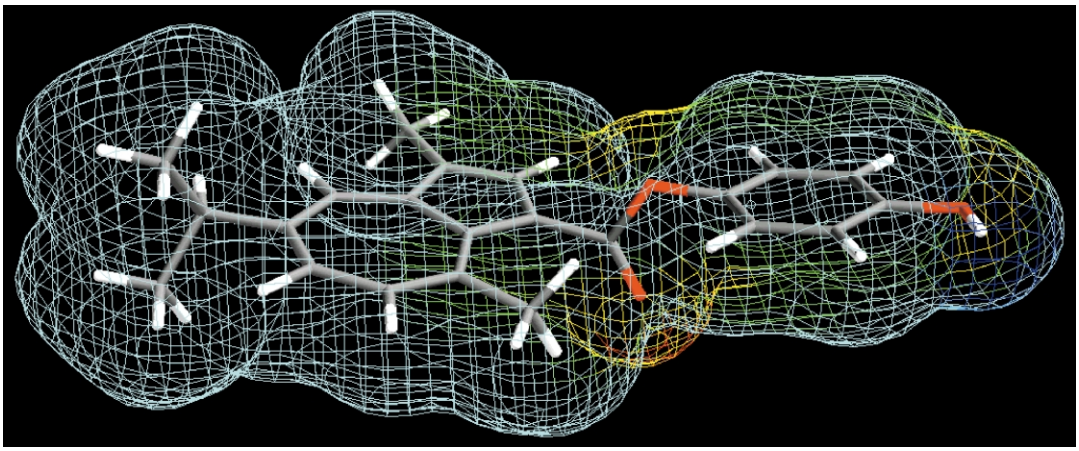

Figure 6. Calculated electrostatic potential surface of **4a** (the electrostatic potential decreases on going from blue to red lines).

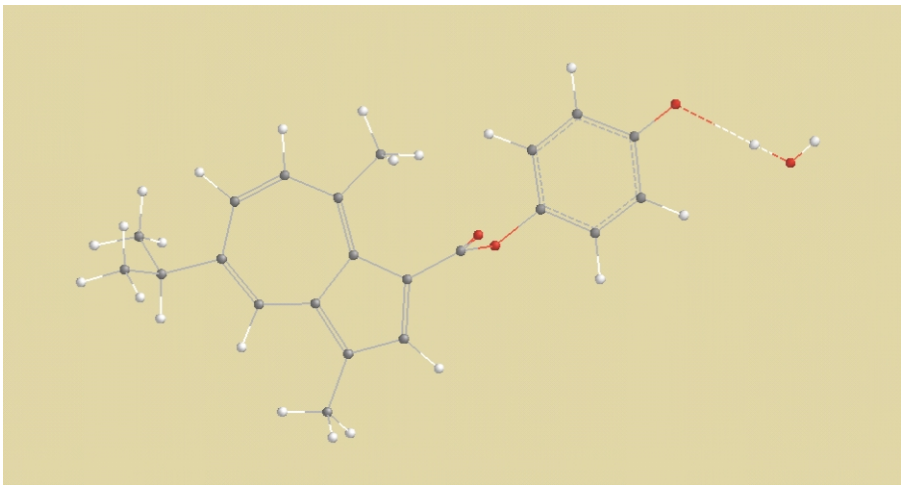

Figure 7. Representation of the calculated transition state geometry for the reaction between **4a** and the hydroxyl radical.

almost independently of the substitution on the phenolic ring. In particular, the most positive electrostatic potential (blue coloured iso-potential lines) is over the phenol hydroxylic hydrogen while the most negative one (red coloured iso-potential lines) is near the ester bond (Fig. 6).

The DFT energy profile of the reaction between **4a** and the hydroxyl radical was calculated and the activation energy value (E_a=9.5 kcal mol^{-1}) and the transition state were thus obtained. The calculated data confirms that the position of the attack by the radical species to the phenolic group (Fig. 7) is in a good agreement with the transition state reported in the literature[30] for the hydrogen abstraction reaction from a generic phenol derivative by a peroxyl radical.

As far as the evolution of the phenoxyl radicals derived from the compounds **4** is concerned, significant information comes from some theoretical and experimental data. According to the calculated geometries of **4i** and **8**, it can be observed that the C(1)–O(2) bond length increases and the O(2)–C(3) bond length decreases, on going from **4i** to the corresponding phenoxyl radical **8** (Fig. 8). This, in conjunction with the EPR data, seems to suggest the radical fragmentation pathway shown in Scheme 3, according to which the phenoxyl radical **8** derived from **4i** could release 2,5-di-*tert*-butylquinone **9**, in addition to unidentified species. Indeed, TLC of the organic extracts of the reaction of **4i** with the H_2O_2/Cu(II) system revealed the presence of **9** along with other unidentified products.

According to the reactions outlined in Scheme 3, we are strongly inclined to conclude that the transient red colour observed when compounds **4** react with oxygen-centred radicals might be associated with the phenoxyl radical, although we did not succeed in obtaining a UV–vis spectrum of any of these radicals owing to their short lifetime. Analogously, we did not succeed in identifying the products resulting from the radicalic degradation of compounds **4**.

3. Conclusions

As hypothesised, the phenol derivatives **4** indeed exhibit chromotropic behaviour on reaction with oxygen-centred radicals, the observed colour variations being due to the oxidative degradation of the starting compounds. Their peroxyl radical scavenging activity is markedly influenced by the nature of the substituents present on the phenolic ring

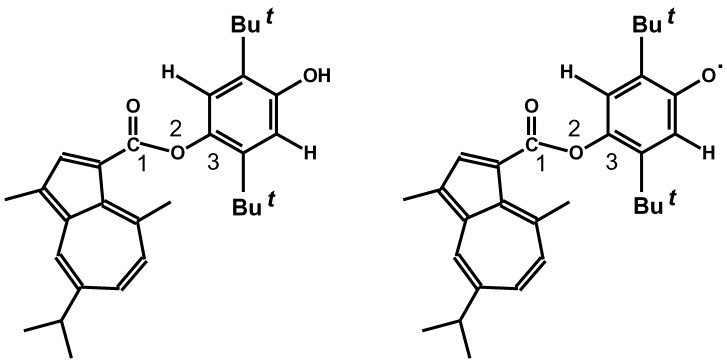

4i **8**

C(1)-O(2) = 1.3765 Å C(1)-O(2) = 1.3803 Å

O(2)-C(3) = 1.3961 Å O(2)-C(3) = 1.3841 Å

Figure 8. Comparison of some calculated bond lengths of **4i** and **8**.

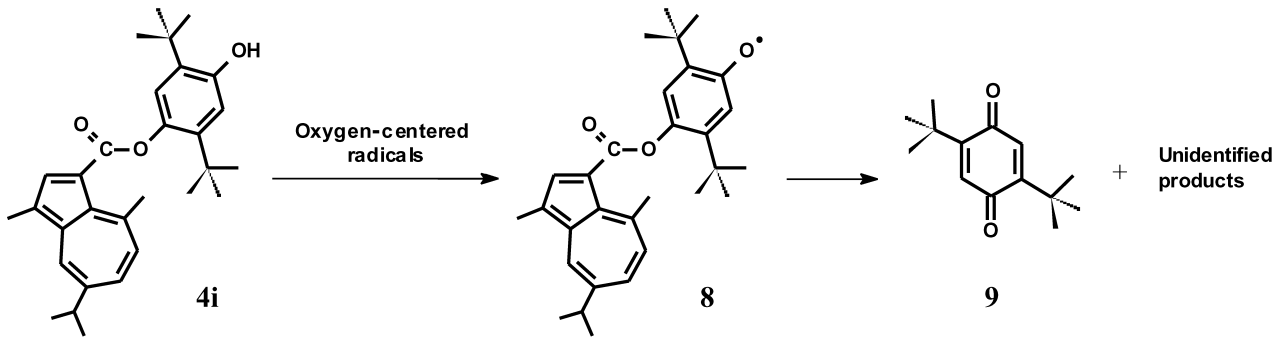

4i **8** **9**

Scheme 3.

as well as by the reaction medium and the nature of the radical partner. In particular, the compounds **4** carrying unsubstituted phenolic rings are less active than those containing alkyl-substituted phenolic rings, and those carrying at least one *ortho*-alkyl group result to be the most active. As stated above, the reaction medium plays a very important role in influencing the scavenging activity of the compounds **4**, which decreases on going from organic solvents to micellar media. For instance, **4a** is a very poor radical scavenger in SDS micelles, while it is as active as BHT in cumene solution. This is quite a general trend in this field.[20,23,31]

It must be underlined that, although the efficiency of compounds **4** has resulted to be lower than that of BHT and α-tocopherol in scavenging the typical oxygen-centred radicals occurring in the oxidation of organic substrates, they exhibit a markedly selective behaviour. Indeed, they react much fast with the hydroxyl radical than with the superoxide radical, this difference being much more marked than that observed in the case of commonly employed antioxidants. As for the reaction of **4a**–**4j** with the hydroxyl radical, the rate is scarcely influenced by structure of the phenolic ring, with the only exception being the reaction with the fluoro-substituted compound **4j**. In this connection, it must be underlined that some of the compounds **4a**–**4j** are as powerful as BHT on reaction with the hydroxyl radical.

The observed antioxidant activity, at least for **4a**,**4c**,**4i** and **4j**, is quite interestingly in perfect accordance with the corresponding phenolic O–H bond dissociation energy. Indeed, this results to be higher in the case of **4a**,**4c** and **4j**, which show moderate to low antioxidant activities, and lower in the case of the most efficient one, i.e. **4i**.

Finally, some aspects of the reaction of the compounds **4** with oxygen-centred radicals have been elucidated. In particular, it has been shown that such compounds transfer their hydroxylic hydrogen to the reacting oxygen-centred radical, as already observed for most of the phenol-based antioxidants, which results in the formation of the corresponding phenoxyl radicals. These last, in turn, undergo a fragmentation reaction which produces the corresponding quinone derivative. The DFT calculation of the transition state of the reaction between compound **4a** and the hydroxyl radical not only gives further grounding to the hydroxylic hydrogen transfer process but also allows an evaluation of the activation energy for such a process.

The comparison of the calculated electrostatic potential

surfaces of the compounds **4** and of two non-guaiazulenic derivatives, **6** and **7**, which carry a phenolic or naphthylic moiety, respectively, instead of the guaizulenic one, allowed us to rationalize the different behaviour exhibited by the two classes of compounds. Interestingly, this means that the presence of the guaiazulenic moiety not only confers chromotropic behaviour to the derivatives **4** but also makes their ester bond less prone to hydrolysis, according to the experimental data. As a final remark we would underline that several aspects of the oxidative degradation of the compounds **4** are still obscure. Thus, our research efforts are now directed to try to clarify these aspects.

4. Experimental

4.1. General

The elemental analysis were performed by the Micro-analysis Laboratory (Facoltà di Farmacia, Pisa, Italy). Melting points were determined by MEL-TEMP II apparatus. ^{1}H NMR spectra were run at 200 MHz by a Varian Gemini 200 instrument or by a Varian VXR 300 instrument, using TMS as internal standard. The Ionspray mass spectra (IS-MS) were recorded by using a mass spectrometer Perkin–Elmer SCIEX API III plus (SCIEX Co., Thornhill, ONT, Canada). Spectrophotometric UV–vis measurements for the inhibition of the autoxidation of linoleic acid were recorded on a Perkin–Elmer Lamba 9 UV/VIS spectrophotometer. Spectrophotometric VIS measurements for the deoxyribose method were recorded on a Jasco Uvidec 710 spectrophotometer UV/VIS. The measurements based upon the Oxygen Up-take Method were carried out at the Department of Organic Chemistry 'A. Mangini', University of Bologna (Italy), by using the apparatus built up in that laboratory.[32]

All the solvents were dried or freshly distilled following the standard procedures. All the purification procedures, which were done by column chromatography, were executed analysing all the fractions by TLC. All chemicals were used as received from Aldrich unless otherwise stated. Bis(ethylenediamine)copper(II) perchlorate was prepared as described.[8] The ethanol and the methanol used in the spectrophotometric measurements were spectrophotometric grade.

The X-band EPR spectra were obtained on a Varian E112 spectrometer. The temperature of the samples was controlled by a Varian E257 temperature control unit. The EPR spectrometer was interfaced to a IPC 610/P566C industrial grade Advantech computer by means of a home made data-acquisition system consisting of an acquisition board capable of acquiring up to 500000 12-bit samples per second including 32-bit add to memory, thus giving on-line signal averaging,[33] and a software package specially designed for EPR experiments.[34] The EPR spectra were run by placing the sample into quartz tubes fitted with a quartz-Pyrex joint and a Bibby Quickfit Rotaflo PTFE tap (Disa, Milan) or Standard TE_{102} Cavity Aqueous Cells (Wilmad) and were recorded according to already published procedures.[35] Water used in the EPR experiments (MILLIPORE MilliQ grade) was first distilled from $KMnO_4$ through a 1 m long Todd column and then saturated with argon, at 20°C for 2 h.

4.2. Computational details

Full optimisation of the geometry of the radical species and calculation of the spin density surfaces, electrostatic potential surfaces and energies were carried out using the UNIX version of Spartan 5.1 computer program,[27] running on a Digital/Compaq workstation, by adopting the p-BP86 scheme that uses the functional proposed by Becke[29] and the Perdew's correlation functional, adopting the DN** base functions set, appropriate for isotropic hfcc calculations of split-valence-polarisation quality.

4.3. General procedure for the preparation of compounds 4a–4j

A solution of oxalyl bromide (0.6 g, 2.7 mmol) in dry diethyl ether (5 ml) was added to a solution of guaiazulene (0.5 g, 2.5 mmol) in diethyl ether (25 ml), at 0°C, under dinitrogen atmosphere. After 10 min, the mixture was allowed to warm at room temperature. After 2 h, 70 ml of diethyl ether were added to the above mixture and the new solution was added drop wise to a solution of the appropriate dihydrobenzene derivative (5 mmol) in diethyl ether (170 ml), at −20°C. The resulting mixture was stirred at room temperature for 12 h. Afterwards, it was treated with 30 ml of a 15% $NaHCO_3$ solution and with solid $NaHCO_3$ until neutral. The aqueous phase was extracted with benzene (2×50 ml) and the extracts were combined with the ethereal solution. The new mixture was dried over Na_2SO_4 and dried under reduced pressure. A microcrystalline solid was obtained in all cases. The purification of crude products was carried out by column (internal diameter, 25 mm; length, 500 mm) chromatography of silica gel 60 (230–400 mesh) (Merck) or of aluminium oxide 90 (70–230 mesh) (Merck) by using the appropriate eluant as specified in the sections below.

4.3.1. 1,4-Dimethyl-3-(4-hydroxyl-1-carbophenoxy)-7-isopropylazulene (4a). The crude reaction product was purified by column chromatography on silica gel using a 7/3 (v/v) diethyl ether/*n*-hexane mixture as the eluant. Pure **4a** (0.34 g, 40%) and the diester **5a** (0.04 g, 6%) were obtained as blue-violet solids.

^{1}H NMR of **4a** (R^1=R^2=R^3=R^4=H) (200 MHz, $CDCl_3$, Me_4Si): δ 1.37 (6H, d, J=6.8 Hz, H^a); 2.61 (3H, s, H^d); 3.05 (3H, s, H^m); 3.12 (1H, m, J=6.8 Hz, H^b); 4.92 (1H, s, OH); 6.95 (4H, m, R^1–R^4); 7.33 (1H, d, J=11.0 Hz, H^n); 7.58 (1H, dd, J=11.0, 2.1 Hz, H^o); 8.17 (1H, s, H^e); 8.27 (1H, d, J=2.1 Hz, H^c). Anal. calcd for $C_{22}H_{22}O_3$ **4a** (344.41): C, 79.0; H, 6.6%. Found: C, 78.9; H, 6.6%. Mp 175–176°C. ν_{max} (KBr) 1711 (CO), 3415 (OH) cm^{-1}.

^{1}H NMR of **5a** (R^1=R^2=R^3=R^4=H) (200 MHz, $CDCl_3$, Me_4Si): δ 1.37 (12H, d, J=6.8 Hz, H^a,); 2.61 (6H, s, H^d); 3.05 (6H, s, H^m); 3.13 (2H, m, J=6.8 Hz, H^b); 7.30 (4H, s, R^1–R^4); 7.36 (2H, s, H^n); 7.57 (2H, dd, J=11.0, 2.1 Hz, H^o); 8.19 (2H, s, H^e); 8.28 (2H, d, J=2.1 Hz, H^c) ppm. Anal. calcd for $C_{38}H_{38}O_4$ **5a** (558.72): C, 81.7; H, 6.9%. Found: C, 81.8; H, 6.9%. Mp>250°C (dec.). ν_{max} (KBr) 1720 (CO) cm^{-1}.

4.3.2. 1,4-Dimethyl-3-(3-hydroxyl-1-carbophenoxy)-7-isopropylazulene (4b). The crude product was purified by column chromatography on silica gel using a 9/1 (v/v) benzene/ethyl acetate mixture as the eluant. Pure **4b** (0.36 g, 43%) and the diester **5b** (ca. 4%) were obtained as blue-violet solids.

^{1}H NMR of **4b** (200 MHz, $CDCl_3$, Me_4Si): δ 1.10 (6H, d, J=6.8 Hz, H^a); 2.38 (3H, s, H^d); 2.72 (1H, m, J=6.8 Hz, H^b); 3.07 (3H, s, H^m); 4.79 (1H, s, OH); 6.50 (1H, m, H^l); 6.78–7.10 (5H, m, H^f, H^g, H^h, H^n, H^o); 8.11 (1H, d, J=2 Hz, H^c); 8.30 (1H, s, H^e) ppm. Anal. calcd for $C_{22}H_{22}O_3$ **4b** (334.41): C, 78.8; H, 6.6%. Found: C, 79.0; H, 6.6%. Mp 126–127°C. ν_{max} (KBr) 1678 and 1712 (CO), 3384 (OH) cm^{-1}.

^{1}H NMR of **5b** (200 MHz, $CDCl_3$, Me_4Si): δ 1.15 (12H, d, J=6.7 Hz, H^a); 2.42 (6H, s, H^d); 2.72 (2H, m, J=6.7 Hz, H^b); 3.10 (6H, s, H^m); 6.82–7.25 (8H, m, H^f, H^g, H^h, H^n, H^o); 8.13 (2H, d, J=2.1 Hz, H^c); 8.32 (2H, s, H^e) ppm. Anal. calcd for $C_{38}H_{38}O_4$ **5b** (558.72): C, 81.7; H, 6.9%. Found: C, 81.7; H, 6.8%. Mp>250°C (dec.). ν_{max} (KBr) 1716 (CO) cm^{-1}.

4.3.3. 1,4-Dimethyl-3-(2-hydroxyl-1-carbophenoxy)-7-isopropylazulene (4c). The crude product was purified by column chromatography on silica gel using a 9/1 (v/v) benzene/ethyl acetate mixture. **4c** (0.4 g, 48%) and the diester **5c** (ca. 4%) were obtained as a blue-violet solids.

^{1}H NMR of **4c** (200 MHz, $CDCl_3$, Me_4Si): δ 1.11 (6H, d, J=6.8 Hz, H^a); 2.35 (3H, s, H^d); 2.70 (1H, m, J=6.8 Hz, H^b); 3.05 (3H, s, H^m); 6.05 (1H, s, H^l); 6.7–7.3 (6H, m, H^f, H^g, H^h, H^i, H^n, H^o); 8.10 (1H, d, J=2.1 Hz, H^c); 8.23 (1H, s, H^e) ppm. Anal. calcd for $C_{22}H_{22}O_3$ **4c** (344.41): C, 79.0; H, 6.6%. Found: C, 78.8; H, 6.6%. Mp 105–106°C. ν_{max} (KBr) 1685 (CO), 3379 (OH) cm^{-1}.

^{1}H NMR of **5c** (200 MHz, $CDCl_3$, Me_4Si): δ 1.24 (12H, d, J=6.9 Hz, H^a); 2.54 (6H, s, H^d); 2.71 (6H, s, H^m); 2.95 (2H, m, J=6.9 Hz, H^b); 6.68 (4H, m, H^f, H^g); 6.90 (2H, d, J=11.0 Hz, H^n); 7.30 (2H, dd, J=11.0, 2.1 Hz, H^o); 7.5 (2H, s, H^e); 8.08 (2H, d, J=2.1 Hz, H^c) ppm. Anal. calcd for $C_{38}H_{38}O_4$ **5c** (558.72): C, 81.7; H, 6.9%. Found: C, 81.8; H, 6.9%. Mp>250°C (dec.). ν_{max} (KBr) 1712 (CO) cm^{-1}.

4.3.4. 1,4-Dimethyl-3-(3-methyl-4-hydroxyl-1-carbophenoxy)-7-isopropyl-azulene (4d) and 1,4-dimethyl-3-(2-methyl-4-hydroxyl-1-carbophenoxy)-7-isopropylazulene (4e). Both these compounds were purified by column chromatography on silica gel using a 9/1 (v/v) benzene/ethyl acetate mixture as the eluant. **4d** (0.27 g, 31%) and **4e** (0.24 g, 28%) were obtained as blue-violet solids.

^{1}H NMR of **4d** (R^1=R^3=R^4=H, R^2=CH_3) (200 MHz, $CDCl_3$, Me_4Si): δ 1.11 (6H, d, J=7.0 Hz, H^a); 2.03 (3H, s, R^2); 2.42 (3H, s, H^d); 2.70 (1H, m, J=7.0 Hz, H^b); 3.12 (3H, s, H^m); 4.39 (1H, s, OH); 6.37 (1H, d, J=11 Hz, H^o); 6.85–7.15 (4H, m, H^n, R^1, R^3, and R^4); 8.12 (1H, s, H^c); 8.39 (1H, s, H^e) ppm. Anal. calcd for $C_{23}H_{24}O_3$ **4d** (348.44): C, 79.31; H, 6.8%. Found: C, 79.4; H, 6.7%. Mp 146–147°C. ν_{max} (KBr) 1657 and 1729 (CO), 3361 (OH) cm^{-1}.

^{1}H NMR of **4e** (R^1=CH_3, R^2=R^3=R^4=H) (200 MHz, $CDCl_3$, Me_4Si): δ 1.12 (6H, d, J=7.0 Hz, H^a); 2.19 (3H, s, R^1); 2.42 (3H, s, H^d); 2.69 (1H, m, J=7.0 Hz, H^b); 3.12 (3H, s, H^m); 4.82 (1H, s, OH); 6.47 (1H, d, J=11 Hz, H^o); 6.82–7.13 (4H, m, H^n, R^2–R^4); 8.11 (1H, s, H^c); 8.40 (1H, s, H^e) ppm. Anal. calcd for $C_{23}H_{24}O_3$ **4e** (348.44): C, 79.31; H, 6.8%. Found: C, 79.4; H, 6.8%. Mp 136–137°C. ν_{max} (KBr) 1682 (CO), 3385 (OH) cm^{-1}.

4.3.5. 1,4-Dimethyl-3-(4-hydroxyl-3-*tert*-butyl-1-carbophenoxy)-7-isopropyl-azulene (4f) and 1,4-dimethyl-3-(4-hydroxyl-2-*tert*-butyl-1-carbophenoxy)-7-isopropylazulene (4g). Both these compounds were purified by column chromatography on silica gel using a 9/1 (v/v) benzene/ethyl acetate mixture as the eluant. The desired monoesters **4f** (0.3 g, 30%) and 4 g (0.1 g, 10%) and the diester **5f** (ca. 5%) were obtained as blue-violet solids.

^{1}H NMR of **4f** (R^1=R^3=R^4=H, R^2=Bu^t) (200 MHz, $CDCl_3$, Me_4Si): δ 1.16 (6H, d, J=7 Hz, H^a); 1.49 (9H, s, R^2); 2.45 (3H, s, H^d); 2.75 (1H, m, J=7 Hz, H^b); 3.17 (3H, s, H^m); 4.17 (1H, s, OH); 6.10 (1H, d, J=8.4 Hz, R^3); 6.90 (1H, d, J=11 Hz, H^n); 7.12 (1H, dd, J=8.4, 2.6 Hz, R^4); 7.40 (1H, d, J=2.6 Hz, R^1); 8.18 (1H, d, J=2 Hz, H^c); 8.42 (1H, s, H^e) ppm. Anal. calcd for $C_{26}H_{30}O_3$ **4f** (390.52): C, 79.9; H, 7.7%. Found: C, 80.0; H, 7.7%. Mp 158–159°C. ν_{max} (KBr) 1697 (CO), 3439 (OH) cm^{-1}.

^{1}H NMR of **4g** (R^1=Bu^t, R^2=R^3=R^4=H) (200 MHz, $CDCl_3$, Me_4Si): δ 1.16 (6H, d, J=7 Hz, H^a); 1.50 (9H, s, R^1); 2.40 (3H, s, H^d); 2.70 (1H, m, J=7 Hz, H^b); 3.15 (3H, s, H^m); 4.32 (1H, s, OH); 6.40 (1H, dd, J=8.7, 3.0 Hz, R^2); 6.80 (1H, d, J=3 Hz, R^3); 6.90 (1H, d, J=11 Hz, H^n); 8.10 (1H, d, J=2 Hz, H^c); 8.45 (1H, s, H^e) ppm. Anal. calcd for $C_{26}H_{30}O_3$ **4g** (390.52): C, 79.9; H, 7.7%. Found: C, 80.1; H, 7.7%. Mp 172–173°C. ν_{max} (KBr) 1698 (CO), 3447 (OH) cm^{-1}.

^{1}H NMR of **5f** (R^1=R^3=R^4=H, R^2=Bu^t) (200 MHz, $CDCl_3$, Me_4Si): δ 1.12 (12H, d, J=7 Hz, H^a); 1.47 (9H, s, R^2); 2.42 (6H, s, H^d); 2.70 (2H, m, J=7 Hz, H^b); 3.16 (6H, s, H^m); 6.93 (2H, d, J=11 Hz, H^n), 6.95–7.60 (4H, m, R^1, R^3, R^4, H^o); 8.13 (2H, d, J=2 Hz, H^c); 8.45 (2H, s, H^e) ppm. Anal. calcd for $C_{42}H_{46}O_4$ **5f** (614.82): C, 82.0; H, 7.5%. Found: C, 81.8; H, 7.6%. Mp>250°C (dec.). ν_{max} (KBr) 1715 (CO) cm^{-1}.

4.3.6. 1,4-Dimethyl-3-(2,3-dimethyl-4-hydroxyl-1-carbophenoxy)-7-iso-propylazulene (4h). The crude product was dissolved in the minimum amount of *n*-hexane and purified by column chromatography on Alumina. The column was eluted first with *n*-hexane, which allowed the separation of the unreacted guaiazulene, then with a 1/1 (v/v) benzene/ethyl acetate mixture, which yielded the diester 5 h as blue crystals (0.160 g, 22%), then with benzene, which allowed to separate the unreacted hydroquinone and, finally, with ethyl formate, which yielded 4 h as a crystalline blue solid (0.362 g, 27%).

^{1}H NMR of **4h** (R^1=R^2=CH_3, R^3=R^4=H) (200 MHz,

$CDCl_3$, Me_4Si): δ 1.37 (6H, d, J=6.8 Hz, H^a); 2.17 (3H, s, R^2); 2.18 (3H, s, R^1); 2.62 (3H, s, H^d); 3.10 (3H, s, H^m); 3.12 (1H, m, J=6.8 Hz, H^b); 4.69 (1H, s, OH); 6.65 (1H, d, J=8.9 Hz, R^3); 6.95 (1H, d, J=8.9 Hz, R^4); 7.33 (1H, d, J=11.0 Hz, H^n); 7.57 (1H, dd, J=11.0, 2.1 Hz, H^o); 8.23 (1H, s, H^e); 8.28 (1H, d, J=2.1 Hz, H^c) ppm. Anal. calcd for $C_{24}H_{26}O_3$ **4h** (362.47): C, 79.5; H, 7.2%. Found: C, 79.5; H, 7.2%. Mp 163–164°C. ν_{max} (KBr) 1690 (CO), 3424 (OH) cm^{-1}.

^1H NMR of **5h** (R^1=R^2=CH_3, R^3=R^4=H) (200 MHz, $CDCl_3$, Me_4Si): δ 1.38 (12H, d, J=6.8 Hz, H^a); 2.24 (6H, s, R^1 and R^2); 2.63 (6H, s, H^d); 3.06 (6H, s, H^m); 3.13 (2H, m, J=6.8 Hz, H^b); 7.10 (2H, s, R^3 and R^4); 7.33 (2H, d, J=11.0 Hz, H^n); 7.58 (2H, dd, J=11.0, 2.1 Hz, H^o); 8.23 (2H, s, H^e); 8.28 (2H, d, J=2.1 Hz, H^c) ppm. Anal. calcd for $C_{40}H_{42}O_4$ **5h** (586.77): C, 81.8; H, 7.2%. Found: C, 81.9; H, 7.2%. Mp>250°C (dec.). ν_{max} (KBr) 1715 (CO) cm^{-1}.

4.3.7. 1,4-Dimethyl-3-(2,5-di-*tert*-butyl-4-hydroxyl-1-carbophenoxy)-7-iso-propylazulene (4i). The crude reaction product was dissolved in the minimum amount of *n*-hexane and purified by column chromatography on aluminium oxide. The column was eluted first with *n*-hexane, which allowed the separation of unreacted guaiazulene, then with a 1/1 (v/v) *n*-hexane/diethyl ether mixture, which yielded the diester **5i** as microcrystalline blue solid (0.192 g, 23%) and, finally, with a 1/1 (v/v) ethyl acetate/diethyl ether mixture, which yielded **4i**, as a microcrystalline blue solid (0.383 g, 35%).

^1H NMR of **4i** (R^1=R^3=H; R^2=R^4=Bu^t) (200 MHz, $CDCl_3$, Me_4Si): δ 1.30–1.33 (24H, m, H^a, R^2, R^4); 2.56 (3H, s, H^d); 2.97 (3H, s, H^m); 3.08 (1H, m, J=6.8 Hz, H^b); 4.72 (1H, s, OH); 6.63 (1H, s, R^3); 6.84 (1H, s, R^1); 7.25 (1H, d, J=11.0 Hz, H^n); 7.51 (1H, dd, J=11.0, 2.1 Hz, H^o); 8.17 (1H, s, H^e); 8.23 (1H, d, J=2.1 Hz, H^c) ppm. Anal. calcd for $C_{30}H_{38}O_3$ **4i** (446.63): C, 80.8; H, 8.5%. Found: C, 80.7; H, 8.5%. EI-MS *m/z*: 446 $[M]^+$. Mp 109–110°C. ν_{max} (KBr) 1687 (CO), 3426 (OH) cm^{-1}.

^1H NMR of **5i** (R^1=R^3=H; R^2=R^4=Bu^t) (200 MHz, $CDCl_3$, Me_4Si): δ 1.42–1.58 (30H, m, H^a, R^2, and R^4); 2.73 (6H, s, H^m); 3.15 (6H, s, H^d); 3.22 (2H, m, J=6.8 Hz, H^b); 7.33 (2H, s, R^1 and R^3); 7.42 (2H, d, J=11.0 Hz, H^n); 7.67 (2H, dd, J=11.0, 2.1 Hz, H^o); 8.33 (2H, s, H^e); 8.39 (2H, d, J=2.1 Hz, H^c) ppm. Anal. calcd for $C_{46}H_{54}O_4$ **5i** (670.93): C, 82.3; H, 8.1%. Found: C, 82.3; H, 8.1%. IS-MS *m/z*: 688 $[M+NH_4]^+$ and 671 $[M+H]^+$. Mp>250°C (dec.). ν_{max} (KBr) 1720 (CO) cm^{-1}.

4.3.8. 1,4-Dimethyl-3-(2,3,5,6-tetrafluoro-4-hydroxyl-1-carbophenoxy)-7-iso-propylazulene (4j). The crude reaction product was dissolved in the minimum amount of *n*-hexane and purified by column chromatography on aluminium oxide, using a 9/1 (v/v) benzene/ethyl formate mixture. **4j** (0.520 g, 51%) and the diester **5j** (ca. 5%) were obtained as blue-violet solids.

^1H NMR of **4j** (R^1=R^2=R^3=R^4=F) (200 MHz, $CDCl_3$, Me_4Si): δ 1.35 (6H, d, J=7 Hz, H^a); 2.61 (3H, s, H^d); 3.04 (3H, s, H^m); 3.15 (1H, m, J=7 Hz, H^b); 6.10 (1H, s, OH); 7.42 (1H, d, J=11.0 Hz, H^n); 7.63 (1H, dd, J=11.0, 2.0 Hz, H^o); 8.24 (1H, s, H^e); 8.29 (1H, d, J=2.0 Hz, H^c). ^{19}F NMR of **4j** (C_6D_6, 188.135 MHz, δ from $CFCl_3$): −164.3 (2F, d, J=17 Hz, R^2 and R^3); −156.4 (2F, d, J=17 Hz, R^1 and R^4) ppm. Anal. calcd for $C_{22}H_{18}F_4O_3$ **4j** (406.38): C, 65.0; H, 4.4%. Found: C, 65.1; H, 4.4%. Mp 140–141°C. ν_{max} (KBr) 1698 (CO), 3291 (OH) cm^{-1}.

^1H NMR of **5j** (R^1=R^2=R^3=R^4=F) (200 MHz, $CDCl_3$, Me_4Si): δ 1.10 (12H, d, J=6.9 Hz, H^a); 2.33 (6H, s, H^d); 2.69 (2H, m, J=6.9 Hz, H^b); 3.05 (6H, s, H^m); 6.87 (2H, d, J=11.0 Hz; H^n); 7.08 (2H, dd, J=11.0, 2.0 Hz, H^o); 8.09 (2H, d, J=2.0 Hz, H^c); 8.40 (2H, s, H^e) ppm. Anal. calcd for $C_{38}H_{34}F_4O_4$ **5j** (630.68): C, 72.3; H, 5.4%. Found: C, 72.2; H, 5.4%. Mp 135–136°C. ν_{max} (KBr) 1698 (CO) cm^{-1}.

4.3.9. 4-Hydroxyphenylbenzoate (6). Following the reported procedure,[36] 1.72 ml (15 mmol) of benzoyl chloride were added to a magnetically stirred solution of hydroquinone (1.5 g, 13.6 mmol), under a dry dinitrogen atmosphere. The pH of the mixture was maintained at 8.6 by a 10% NaOH solution while adding benzoyl chloride, in ca. 40 min. The mixture was then extracted with benzene (3×40 ml). The combined extracts were dried over Na_2SO_4 and then evaporated to dryness under reduced pressure. The resulting solid residue was dissolved $CHCl_3$ (10 ml) and purified by column chromatography on Silica gel, using $CHCl_3$ as the eluant. The desired monoester **6** (0.306 g, 10%) was obtained as a white microcrystalline solid from the third band eluted. Mp 162–163°C.[36]

4.3.10. 4-Hydroxyphenyl-1-naphthoate (7). A solution of 1-naphthoyl chloride (0.377 ml, 2.5 mmol) in 100 ml of diethyl ether was added dropwise to a magnetically stirred solution of hydroquinone (0.55 g, 5 mmol) in diethyl ether (200 ml). After 10 min, the mixture was allowed to warm to room temperature. After 1 h, the reaction mixture was treated with triethylamine (0.348 ml, 2.5 mmol) mixture and maintained at room temperature for 48 h. The mixture was then extracted with benzene (100 ml). The organic extract was washed with water (3×100 ml), dried over Na_2SO_4 and then kept to dryness under reduced pressure. A microcrystalline solid was obtained which was dissolved in 8 ml of a 6/4 (v/v) $CHCl_3$/ethyl acetate mixture. Chromatography on Silica gel, using a 6/4 (v/v) $CHCl_3$/ethyl acetate mixture as the eluant, furnished **7** (0.24 g, 36%) (first band).

^1H NMR of **7** (200 MHz, $CDCl_3$, Me_4Si): δ 5.06 (1H, s, H^l); 6.80–7.18 (4H, m, H^h, $H^{h'}$, H^i, $H^{i'}$); 7.48–7.65 (3H, m, H^b, H^e, H^f); 7.90 (1H, d, J=8.6 Hz, H^d); 8.09 (1H, d, J=7.4 Hz, H^c); 8.44 (1H, dd, J=7.3, 1.5 Hz, H^a); 8.99 (1H, d, J=8.4 Hz, H^g) ppm. Anal. calcd for $C_{17}H_{12}O_3$ **7** (264.28): C, 77.3; H, 4.5%. Found: C, 77.3; H, 4.4%. Mp 143–144°C. ν_{max} (KBr) 1697 (CO), 3411 (OH) cm^{-1}.

4.4. Reaction of compounds 4a–4j with H_2O_2 in the presence of $(Cu(en)_2((ClO_4)_2$

0.5 ml of H_2O_2 (2 M, pH 4) were introduced in a test-tube and treated with a solution of the appropriate compound **4** (60 μl) of a 0.01 M solution in sodium decyl sulfate (1 M, pH 9) and then with 50 μl of a 0.01 M solution of $(Cu(en)_2((ClO_4(_2$ in water, at room temperature. In all

cases the mixture became yellow in colour within ca. 15 min. All the mixtures were treated with ethyl formate (0.5 ml) and shaken for a few seconds. The organic layers were then tested by TLC (SiO_2, using benzene/ethyl acetate mixtures in different ratios, depending upon the reactive system).

4.5. Reaction of compounds 4a–4j with KO_2

These reactions were carried out under a dry dinitrogen atmosphere. 0.5 ml of a solution of KO_2 in DMSO (0.1 M) containing 18-crown-6 (0.1 M) were introduced into a test-tube and then treated with 10 μl of a 0.007 M solution of the appropriate compound **4** in DMSO. After 5 min, the reaction mixture was treated with 3 ml of H_2O, 1 ml of ethyl formate and shaken for a few seconds. The organic layer was then tested by TLC (SiO_2, using benzene/ethyl acetate mixtures in different ratios, depending upon the reactive system).

4.6. Inhibition of the autoxidation of linoleic acid

The experiments were carried out according the procedure reported in literature.[12]

Preparation of the solutions. Stock solutions of phosphate buffer (0.3 M, pH 7.4) were prepared and stored in plastic bottles for no more than 2 weeks. The solution of 0.5 M 2,2′-azobis(2-amidinopropane)dihydrochloride (ABAP) was freshly prepared in 0.05 M phosphate buffer (pH 7.4). The stock solution of linoleic acid in sodium *n*-dodecyl sulfate was prepared as follows: 0.692 g of sodium *n*-dodecyl sulfate (SDS) and 20 μl of linoleic acid were dissolved in 20 ml of deareated water under nitrogen atmosphere. The solution was stored in a Carius tube at −18°C. The stock solutions of antioxidants were freshly prepared in absolute ethanol at concentrations of 10^{-3} M.

Autoxidation procedure. In a typical run, the UV cuvette containing 2 ml of linoleic acid in SDS solution and 0.4 ml of phosphate buffer (0.3 M; pH 7.4) was thermostated at 37±0.2°C and stirred continuously in the sample compartment of the spectrophotometer. After about 20 min, when the thermal equilibration in the spectrophotometer was completed, an aliquot (10±0.1 μl) of ABAP 0.25 M was added and incubated for an additional 40 min in order to allow the rate of autoxidation to become constant. An aliquot (10±0.1 μl) of antioxidant solution was then added and the change in absorbance was monitored with time at 234 nm.

4.7. Inhibition of the autoxidation of cumene

4 ml of cumene and 10 μl of a 2×10^{-3} M benzene solution of the appropriate radical scavenger were added to the sample flask; 4 ml of cumene and 20 μl of a 10^{-2} M benzene solution of α-tocopherol were added to the reference flask. Both the flasks were thermostated at 50°C. When the thermal equilibration was completed, an aliquot (40±0.1 μl) of a 0.34 M solution of AIBN in acetonitrile was added to both the flasks and the oxygen up-take was recorded.

4.8. Inhibition of the degradation of deoxyribose

0.2 ml of a solution of $FeSO_4{\cdot}7H_2O$ (10^{-2} M) and EDTA (10^{-2} M) in sodium *n*-dodecyl sulfate (0.1 M), 0.2 ml of 2-deoxyribose solution (10^{-2} M) in sodium *n*-*n*-dodecyl sulfate (0.1 M), 0.4 ml of phosphate buffer solution (0.1 M, pH 7.4) in sodium *n*-dodecyl sulfate (0.1 M) and 1 ml of antioxidant solution (10^{-3} M) in methanol were added to a screw-capped test tube. Finally, 0.2 ml of a H_2O_2 water solution (10^{-2} M) were added and the whole was incubated at 37°C for 4 h. After this incubation, 1 ml of a trichloroacetic acid solution (2.8%) in sodium *n*-dodecyl sulfate (0.1 M) and 1 ml of thiobarbituric acid solution (1%) in NaOH (5×10^{-2} M) in sodium *n*-dodecyl sulfate (0.1 M) were added and the resulting mixture was boiled for 45 min, then cooled in ice and its absorbance measured at 532 nm. Each run was repeated three times.

4.9. Single crystal X-ray structure determination of 1,4-dimethyl-3-(4-hydroxyl-1-carbophenoxy)-7-isopropyl-azulene (4a) and 1,4-dimethyl-3-(3-hydroxyl-1-carbo-phenoxy)-7-isopropylazulene (4b)

The diffractometric measurements were carried out at room temperature by means of a Bruker P4 diffractometer equipped with a graphite-monochromated Mo K_α radiation (λ=0.71073 Å). All data were collected using an $\omega/2\theta$ scan mode, and three standard reflections were monitored every 97 measurements for checking the crystal decay and equipment stability. Data reduction was done by the SHELXTL program. All refinement cycles were done by full-matrix least-squares procedures based on F^2.

Single crystals of **4a** are violet-blue monoclinic tables. One of them with dimensions 0.68×0.48×0.06 mm^3 was glued at the end of a glass fibre. The cell parameters listed in Table 1 were obtained from the setting angles of 42 strong reflections. The upper θ limit of collection was restricted to 21.2° because behind this value the fraction of observed reflections was very low. 2848 reflections, having $-1\leq h\leq5$, $-37\leq k\leq1$, and $-8\leq l\leq8$, were collected. After correction for Lorentz and polarization effects the equivalent reflections were merged giving a set of 2018 independent reflection ($R_{int}=[\sum|F_o^2-F_{o(mean)}^2|/\sum(F_o^2)]=0.0497$). The structure solution was obtained by means of direct methods by using SHELXS-97 program. The hydrogen atoms were introduced in calculated positions and let to ride on the connected carbon atoms. The final refinement cycle gave the reliability factors listed in Table 6.

A crystal with dimensions 0.48×0.20×0.05 mm of a deep red crystal of **4b** was glued at the end a glass fibre. The unit cell parameters together with the space group and some structural details are listed in Table 6. The intensity data of 5769 reflections having $2.28<\theta<22.50$ were collected. After correction for Lorentz, polarization the equivalent reflections were merged giving a total of 4640 independent reflection (R_{int}=0.0972). The structure was solved by standard Patterson and Fourier methods by means of SHELXS-97 program. The final refinement cycles gave the reliability factors listed in Table 6.

Complete crystallographic data for **4a** and **4b** been

Table 6. Crystal data and structure refinement

Compound	**4a**	**4b**
Empirical formula	$C_{22}H_{22}O_3$	$C_{22}H_{22}O_3$
Formula weight	334.40	334.40
Temperature (K)	293(2)	293(2)
Crystal system	Monoclinic	Monoclinic
Space group	$P2_1/n$ (No.14)	$P2_1/c$ (No.14)
Unit cell dimensions		
a (Å)	5.873(1)	27.275(5)
b (Å)	37.216(9)	11.214(3)
c (Å)	8.458(1)	11.826(2)
β (°)	94.28(1)	101.33(1)
Volume (Å^3)	1843.5(6)	3546.6(13)
Z	4	8
ρ_{calc} (Mg m^{-3})	1.205	1.253
μ (mm^{-1})	0.079	0.082
Data/restraints/parameters	2018/0/235	4640/0/453
$R(F_o)$ [$I>2\sigma(I)$]	0.0760	0.0803
R_w (F_o^2) [$I>2\sigma(I)$]	0.1888	0.1739

$R(F_o)=\sum||F_o|-|F_c||/\sum|F_o|$; $R_w(F_o^2)=[\sum[w(F_o^2-F_c^2)^2]/\sum[w(F_o^2)^2]]^{1/2}$; $w=1/[\sigma^2(F_o^2)+(AQ)^2+BQ]$ where $Q=[MAX(F_o^2,0)+2F_c^2]/3$.

deposited, in the form of CIF files, with the Cambridge Crystallographic Data Centre (Dep. No. CCCD 188035 and CCCD 188036, respectively for **4a** and **4b**).

Acknowledgements

We want to express our gratitude to Dr G. Chiaradonna (Procter & Gamble fellowship, University of Pisa, Italy) for the contribution she gave to this work through the preliminary investigation of the synthesis of some guaiazulenic derivatives and the study of their reactivity towards free radicals. We are grateful to Professor G. F. Pedulli (University of Bologna, Italy) for the kind permission to use the oxygen up-take apparatus and Dr R. Amorati for his precious assistance in carrying the oxygen up-take measurements. Moreover, we thank Procter & Gamble Italia S.p.A. (Rome, Italy) and University of Pisa (Italy) for financial support.

References

1. *Handbook of Synthetic Antioxidants*; Packer, L., Cadenas, E., Eds.; Marcel Dekker: New York, 1997.
2. (a) Ingold, K. U. *Chem. Rev.* **1961**, *61*, 562–589. (b) Neri, C. *Chim. Ind.* **1997**, *79*, 1223–1232.
3. (a) Denisov, E. T.; Khudyakov, I. V. *Chem. Rev.* **1987**, *87*, 1313–1357. (b) Foti, M.; Ingold, K. U.; Lusztyk, J. *J. Am. Chem. Soc.* **1994**, *116*, 9440–9447.
4. Becker, D. A. *J. Am. Chem. Soc.* **1996**, *118*, 905–906.
5. (a) Wang, B.; Lin, Y.; Chang, J.; Wang, P. *Can. J. Chem.* **2000**, *78*, 224–232. (b) Liu, R. S. H.; Muthyala, R. S.; Wang, X.; Asato, A. E. *Org. Lett.* **2000**, *2*, 269–271. (c) Razus, A. C. *J. Chem. Soc., Perkin Trans. 1* **2000**, 981–988.
6. (a) Franchi, E.; Ingrosso, G.; Pinzino, C.; Chiaradonna, G.; Cicogna, F.; Del Duca, V.; Scialla, S. *Sixth International Symposium on Spin Trapping*, Marseille, France, 27–31 August 2000, Abstracts, p 135. (b) Franchi, E.; Ingrosso, G.; Pinzino, C.; Chiaradonna, G. 6° *Convegno Nazionale del Gruppo Italiano di Risonanza di Spin Elettronico*, *GIRSE*, Urbino-Sogesta, 17–20 Settembre 2001, Atti del Convegno PS 24. (c) Franchi, E.; Ingrosso, G.; Pinzino, C. 1° *Sigma Aldrich Young Chemists Symposium*, *SAYCS* Riccione, 18–19 Ottobre 2001, Abstracts p PO 49.
7. Chiaradonna, G.; Cicogna, F.; Ingrosso, G.; Pinzino, C.; Franchi, E.; Del Duca, V.; Scialla, S. European Patent EP 1094057 A1, Date of publication 25.04.2001; International Patent Classification: C07C 69/753; International Publication Number: WO 01/28973 A1 (International Publication Date 26.04.2001).
8. Ozawa, T.; Hanaki, A. *J. Chem. Soc., Chem. Commun.* **1991**, 330.
9. *Catalytic Oxidation with Hydrogen Peroxide as Oxidant*; Strukul, G., Ed.; Kluwer Academic: Dordrecht, 1992.
10. Kim, S.; Di Cosimo, R.; San Filippo, J. *J. Anal. Chem.* **1979**, *51*, 679–681.
11. Dannacher, J.; Schlenker, W. *Text. Chem. Color.* **1996**, *28*, 24–28.
12. Pryor, W. A.; Cornicelli, J. A.; Devall, L. J.; Tait, B.; Trivedi, B. K.; Witiak, D. T.; Wu, M. *J. Org. Chem.* **1993**, *58*, 3521–3532.
13. Dangles, O.; Dufour, C.; Fargeix, G. *J. Chem. Soc., Perkin Trans. 2* **2000**, 1215–1222.
14. Howard, J. L.; Ingold, K. U. *Can. J. Chem.* **1969**, *47*, 3809–3815.
15. Halliwell, B.; Gutteridge, J. M. C.; Aruoma, O. I. *Anal. Biochem.* **1987**, *165*, 215–219.
16. Chung, S.; Osawa, T.; Kawakishi, S. *Biosci. Biotechnol. Biochem.* **1997**, *61*, 118–123.
17. *Molecular Biology of Free Radicals in Human Diseases*; Aruoma, O. I., Halliwell, B., Eds.; OICA International: Saint Lucia, London, 1998.
18. (a) Bordwell, F. G.; Cheng, J. *J. Am. Chem. Soc.* **1991**, *113*, 1736–1743. (b) Burton, G. W.; Doba, T.; Gabe, E. J.; Hughes, L.; Lee, F. L.; Prasad, L.; Ingold, K. U. *J. Am. Chem. Soc.* **1985**, *107*, 7053–7065. (c) Brinck, T.; Haeberlein, M.; Jonsson, M. *J. Am. Chem. Soc.* **1997**, *119*, 4239–4244. (d) Franchi, P.; Lucarini, M.; Pedulli, G. F.; Valgimigli, L.; Lunelli, B. *J. Am. Chem. Soc.* **1999**, *121*, 507–514.
19. Barclay, L. R. C.; Baskin, K. A.; Locke, S. J.; Vinqvist, M. R. *Can. J. Chem.* **1989**, *67*, 1366–1369.
20. Pryor, W. A.; Strickland, T.; Church, D. F. *J. Am. Chem. Soc.* **1988**, *110*, 2224–2229.
21. (a) Burton, G. W.; Ingold, K. U. *J. Am. Chem. Soc.* **1981**, *103*, 6472–6477. (b) Denisov, E. T.; Azatin, V. V. *Inhibition of Chain Reactions*; Gordon & Breach: London, 2000.
22. Amorati, R. PhD Thesis, University of Bologna, Italy, 1998–1999.
23. Valgimigli, L.; Ingold, K. U.; Lusztyk, J. *J. Am. Chem. Soc.* **1996**, *118*, 3545–3549.
24. (a) Lucarini, M.; Pedulli, G. F.; Cipollone, M. *J. Org. Chem.* **1994**, *59*, 5063–5070. (b) Yamamura, T.; Suzuki, K.; Yamaguchi, T.; Nishiyama, T. *Bull. Chem. Soc. Jpn* **1997**, *70*, 413–419. (c) Bordwell, F. G.; Zhang, X.; Satish, A. V.; Cheng, J. *J. Am. Chem. Soc.* **1994**, *116*, 6605–6610. (d) Brink, T.; Haeberlein, M.; Jonsson, M. *J. Am. Chem. Soc.* **1997**, *119*, 4239–4244.
25. (a) Migliavacca, E.; Carrupt, P.; Testa, B. *Helv. Chim. Acta* **1997**, *80*, 1613–1626. (b) Migliavacca, E.; Ancerewicz, J.; Carrupt, P.; Testa, B. *Helv. Chim. Acta* **1998**, *81*, 1337–1348.
26. Denisov, E. T.; Denisova, T. G. *Handbook of Antioxidants*; CRC: Cleveland, OH, 2000.
27. Spartan version 5.1; Wavefunction, Inc.: 18401 Von Karman Avenue, Suite 370 Irvine, CA 92612, USA.

28. Duling, D. R. *J. Magn. Reson. B* **1994**, *104*, 105–110.
29. Becke, A. D. *J. Chem. Phys.* **1993**, *98*, 1372–1377.
30. (a) Tanaka, K.; Sakai, S.; Tomiyama, S.; Nishiyama, T.; Yamada, F. *Bull. Chem. Soc. Jpn* **1991**, *64*, 2677–2680. (b) Tomiyama, S.; Sakai, S.; Nishiyama, T.; Yamada, F. *Bull. Chem. Soc. Jpn* **1993**, *66*, 299–304.
31. (a) Barclay, L. R. C.; Edwards, C. D.; Mukai, K.; Egawa, Y.; Nishi, T. *J. Org. Chem.* **1995**, *60*, 2739–2744. (b) Castle, L.; Perkins, M. J. *J. Am. Chem. Soc.* **1986**, *108*, 6381–6382. (c) Barclay, L. R. C.; Baskin, K. A.; Dakin, K. A.; Locke, S. J.; Vinqvist, M. R. *Can. J. Chem.* **1990**, *68*, 2258–2269. (d) MacPaul, P. A.; Ingold, K. U.; Lusztyk, J. *J. Org. Chem.* **1996**, *61*, 1316–1321. (e) Valgimigli, L.; Banks, J. T.; Ingold, K. U.; Lusztyk, J. *J. Am. Chem. Soc.* **1995**, *117*, 9966–9971. (f) Pryor, W. A.; Kaufman, M. J.; Church, D. F. *J. Org. Chem.* **1985**, *50*, 281–283. (g) Barclay, L. R. C.; Edwards, C. D.; Vinquist, M. R. *J. Am. Chem. Soc.* **1999**, *121*, 6226–6231.
32. Pedulli, G. F.; Lucarini, M.; Pedrielli, P. In *Free Radicals in Biology and Environment*; Minisci, F., Ed.; Kluwer Academic: Dordrecht, 1997; pp 169–179.
33. Ambrosetti, R.; Ricci, D. *Rev. Sci. Instrum.* **1991**, *62*, 2281–2287.
34. Pinzino, C.; Forte, C. EPR-ENDOR, ICQEM-CNR Rome, Italy, Copyright 1992–2000.
35. (a) Diversi, P.; Forte, C.; Franceschi, M.; Ingrosso, G.; Lucherini, A.; Petri, M.; Pinzino, C. *J. Chem. Soc., Chem. Commun.* **1992**, 1345–1347. (b) Bruni, M.; Diversi, P.; Ingrosso, G.; Lucherini, A.; Pinzino, C.; Raffaelli, A. *J. Chem. Soc., Dalton Trans.* **1995**, 1035–1041. (c) Bruni, M.; Diversi, P.; Ingrosso, G.; Lucherini, A.; Pinzino, C. *Gazz. Chim. Ital.* **1996**, *126*, 239–250. (d) Carano, M.; Careri, M.; Cicogna, F.; D'Ambra, I.; Houben, J. L.; Ingrosso, G.; Marcaccio, M.; Paolucci, F.; Pinzino, C.; Roffia, S. *Organometallics* **2001**, *20*, 3478–3490. (e) Carano, M.; Cicogna, F.; Houben, J. L.; Ingrosso, G.; M.archetti, F.; Mottier, L.; Paolucci, F.; Pinzino, C.; Roffia, S. *Inorg. Chem.* **2002**, *41*, 3396–3409. (f) Carano, M.; Cicogna, F.; D'Ambra, I.; Gaddi, B.; Ingrosso, G.; Marcaccio, M.; Paolucci, D.; Paolucci, F.; Pinzino, C.; Soffia, S. *Organometallics* **2002**, *21*, 5583–5593.
36. Bredereck, H.; Heck, H. *Chem. Ber.* **1958**, *91*, 1314–1318.